

Effects of anchorage deterioration on the shear behaviour of reinforced concrete half-joint beams

Citation:

Mak, M.W.T., Sheasby M.P. and Lees, J.M. (2020). Effects of anchorage deterioration on the shear behaviour of reinforced concrete half-joint beams. *Proceedings of the fib Symposium 2020 on Concrete Structures for Resilient Society*. 22-24 Nov 2020, Shanghai, China.

Version:

Accepted for publication

Please cite the published version.

EFFECTS OF ANCHORAGE DETERIORATION ON THE SHEAR BEHAVIOUR OF REINFORCED CONCRETE HALF-JOINT BEAMS

Michele Win Tai MAK¹, Matthew P. SHEASBY², Janet M. LEES³

1. PhD Candidate, Department of Engineering, University of Cambridge, Cambridge, United Kingdom

2. Engineer, COWI, London, United Kingdom

3. Professor, Department of Engineering, University of Cambridge, Cambridge, United Kingdom

Corresponding author email: mwtm2@cam.ac.uk

Abstract

Reinforced concrete half-joint structures, also called dapped-end beams, are a common type of support configuration in bridges and precast structures. They are characterised by a sudden reduction in depth at the end of a suspended structural element. This detail has advantages for design and construction that justified their widespread use in the past. However, there are numerous problems associated with this type of joint that can translate into significant maintenance costs. A recurrent issue is leakage of water and contaminants that cause corrosion of the internal steel reinforcement. The expansive nature of corrosion products can lead to cracking, delamination or complete spalling of the concrete cover. This is detrimental to the anchorage of the reinforcement. The subsequent reduction in load-transfer capacity is difficult to quantify when assessing damaged structures. It can lead to failure modes that are not taken into account by code provisions for new design. Due to the limited understanding of the behaviour of deteriorated half-joints, experimental evidence is necessary to develop new theories and methodologies to assess existing structures accurately. In this study, an experimental programme was carried out on reinforced concrete beam specimens, investigating the effects of anchorage deterioration in the longitudinal tension bars of the full-depth portion of half-joints. Corrosion-induced spalling and delamination were reproduced by casting the beams without cover and reducing the cover/diameter ratio at critical locations. The results indicate that half-joints are vulnerable to anchorage deterioration in the full-depth section. This is due to the absence of direct confining pressure from the end supports. Bond and anchorage degradation led to a progressive reduction in the overall load-bearing capacity of the beam-ends and combined bending-shear failure modes. Nevertheless, the presence of confining vertical reinforcement allowed for some residual anchorage capacity, even in the case of complete loss of cover.

Keywords: *Bond, corrosion, cracking, dapped-end, spalling.*

1. Introduction

Existing reinforced concrete structures are subjected to several sources of deterioration that can cause a reduction in load-bearing capacity. Assessing their residual resistance is a challenging task for asset managers. This leads to significant costs of inspection, maintenance, repair, strengthening or decommissioning. In extreme situations, this has led to structural failures with tragic consequences for the community (Mitchell et al. 2011, di Prisco et al. 2018). To manage the infrastructure network effectively, identifying priorities is paramount.

Half-joint bridges represent a critical class of infrastructure. A half-joint, also called dapped-end, is a type of simple support, where the depth of a suspended element is reduced at its end (see Figure 1). This configuration has several advantages for design and construction, which led to their widespread use in the past, particularly in highway overpasses. Within the U.K. Highways England network alone, there are currently 424 reinforced concrete half-joint bridges in use (Desnerck et al. 2018) and many more worldwide. Despite their advantages for design and buildability, there are problems associated

with this type of joint. Among them is leakage of water from the bridge surface through the joint seal. De-icing salt from the road can be present in the water, which often stagnates within the half-joint. Contaminated water can cause deterioration and corrosion of the internal steel reinforcement in that region. Due to the expansive nature of corrosion products, this leads to cracking of the concrete cover and complete spalling in extreme cases. An example of a highway half-joint bridge with extensive corrosion-induced spalling is shown in Figure 1.a.

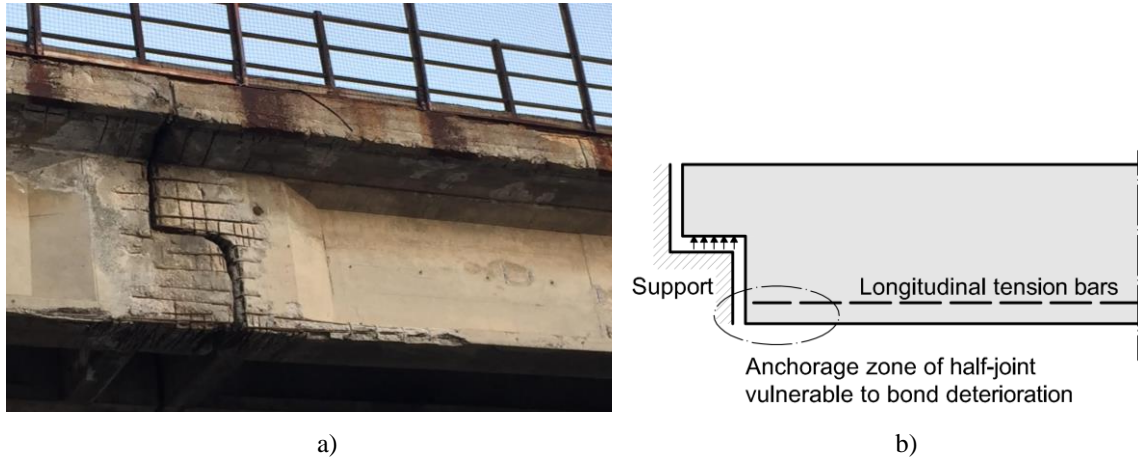


Figure 1. Deterioration of half-joint structures: a) Corrosion-induced spalling in a half-joint overpass; b) Absence of transverse support pressure on the anchorage zone of longitudinal reinforcement in the full-depth section of a half-joint.

In reinforced concrete structures, corrosion of the internal bars leads to a reduction in bond between steel and concrete. Earlier work indicates that concrete cracking is directly related to the bond deterioration mechanism (Mak et al. 2019). In the anchorage zone of straight bars, bond deterioration can lead to a reduction in the overall load-bearing capacity. The anchorage zone of longitudinal tension bars in half-joints is particularly vulnerable to bond deterioration. This is because the underside of the full-depth section is effectively suspended, as shown schematically in Figure 1.b. Unlike conventional simple support configurations, this anchorage zone does not benefit from direct transverse pressure from the support, which would enhance the bond performance (Cairns 2015). This aspect of half-joints has not been studied extensively, especially in relation to the assessment of existing structures which is fundamentally different from the design of new structures. In reinforced concrete design, the steel-to-concrete bond of straight bars relies on the presence of concrete cover around them (*fib* 2000). In the case of delamination and spalling, the reinforcement is no longer fully encased, current theories and models are therefore not valid. New theories and experimental evidence are therefore necessary to develop predictive models.

2. Experimental Programme

The present study focusses on the anchorage deterioration of longitudinal bars in the full-depth section of half-joints. A series of reinforced concrete half-joint beam specimens were tested to investigate the effects of anchorage deterioration on the overall structural behaviour of the components. Bond deterioration was simulated by locally reducing the cover distance on the bottom corner of the full-depth section. The cover depth to the longitudinal reinforcement was varied to mimic a loss of cover due to spalling. The anchorage length of the longitudinal bottom bars was limited to 5 bar diameters using a debonding sleeve. A total of 4 specimens were tested in 3-point bending. The experimental programme was designed to investigate the failure modes induced by anchorage deterioration. The characteristics of the specimens and testing arrangement are shown in Figure 2. In the notation adopted in this study, each half-joint test is identified by the letters *HJ*, followed by the specimen number (1 to 2) and a letter indicating the first or second beam-end test (respectively *a* or *b*), followed by the letter *c* and a number corresponding to the cover distance in millimetres at the critical

location (e.g.: *HJ-2b-c16* indicates the half-joint beam no. 2, the second test out of the two beam-ends, with a cover of 16 mm on the critical node).

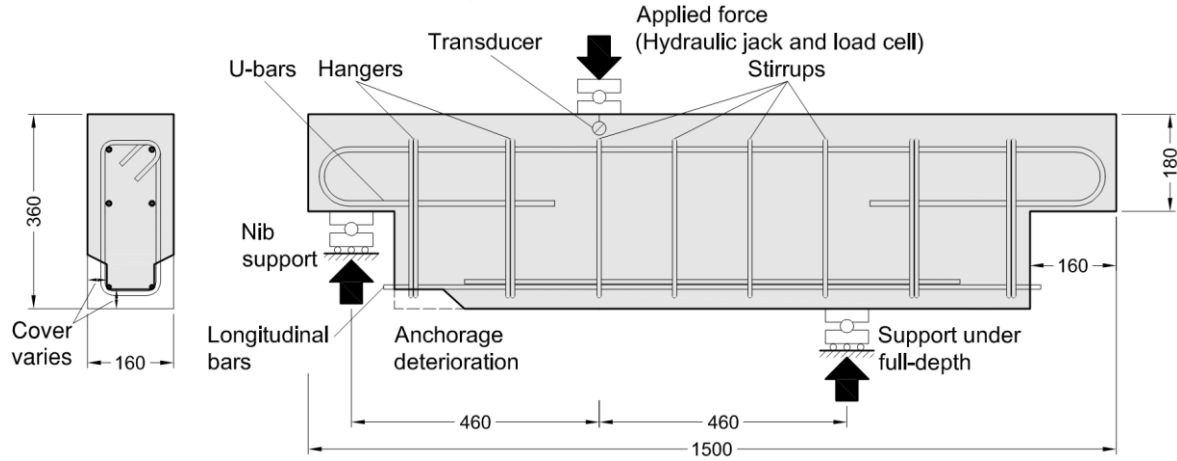


Figure 2. Set-up and reinforcement layout of 3-point bending test. Left half-joint under testing while the right half-joint is unstressed

2.1. Materials

The reinforcement consisted of high-strength steel deformed bars with a nominal yield strength of 500 MPa. The longitudinal bars of the full-depth section were H8. All vertical shear links were H8 bars. In the first two rows of vertical shear links (hanger reinforcement) from the supports, the stirrups were doubled. The flexural U-bar at the nib was a H10. The nib was over-reinforced to avoid premature bending failure at that location. To avoid premature bending failure of the beams, the mid-span was over-reinforced with two additional longitudinal tension bars which did not reach the bottom corner of the full-depth section, in order not to affect the anchorage node.

The concrete was a C16/20 Ordinary Portland Cement (OPC) mix with no admixtures. Fine aggregate consisted of river sand, coarse aggregate was uncrushed coarse gravel with a maximum size of 10 mm. The mix composition and proportions of the constituents are summarised in Table 1. Material characterisation tests were carried out at 14 days after casting. On average, the concrete compressive strength measured on 100 mm concrete cubes was $f_{c,cub,14} = 15.6$ MPa with a Standard Deviation (SD) of 0.78 MPa and the split tensile strength measured on cylinders (dia: 100 mm, height: 200 mm) was $f_{ct,sp,14} = 1.57$ MPa (SD: 0.08 MPa). The specimens were cast into plywood formwork, compacted on a vibrating table and immediately covered with plastic sheets. The specimens were removed from the formwork at least 24 hours after casting, covered in plastic sheets and left to cure in an indoor environment. The curing conditions were uncontrolled.

Table 1. Concrete mix composition.

Constituent	Type	Density [kg/m ³]	Amount [kg/m ³]
Water	-	1,000	225
Cement	CEM II-A-LL 32.5 R	3,100	290
Fine aggregate		2,625	730
Coarse aggregate	4/10mm	2,625	1,050

2.2. Specimen geometry and test set-up

The specimens had a total length of 1,500 mm, a width of 160 mm and an overall depth of 360 mm. The nib height of 180 mm was equal to half of the full depth section. The nib length was 160 mm and the support was centred under the nib. The distance between the centre of the support and the centreline of the first row of hanger reinforcement was therefore 115 mm. While one half-joint was being tested, the other support at the opposite end of the beam was located under the full-depth section. This testing configuration (see Figure 2) was chosen to prevent damage of the half-joint that was not being tested. At the end of one experiment, the specimen was rotated and the opposite beam-end was tested under the same conditions. The span between supports was 910 mm. The load was

applied at mid-span with a hydraulic jack and measured with a compression load cell. Strain gauges were installed on the reinforcing bars to measure the strains at critical locations. These locations are shown in Figure 3.b and included the end of the anchorage zone of the longitudinal bars and the lowest portion of the stirrups in the first row of vertical reinforcement. The first set of strain gauges were used to calculate the anchorage force and therefore the bond stresses on the longitudinal bars. Although not presented here, the second set of measurements were used to estimate the stresses in the hanger reinforcement that acted as transverse confinement on the anchorage of longitudinal bars.

2.3. Simulation of spalling and anchorage degradation

Spalling and bond deterioration were simulated by casting the specimens with a progressively reducing cover distance at the bottom corner of the full-depth section. The approach of reducing the concrete cover to study anchorage deterioration has been used previously (Regan and Kennedy Reid 2009, Orr et al. 2017, Mak and Lees 2019). The bottom corner location was considered critical as it corresponded to the anchorage zone of the bottom tension reinforcement of the beams, which was achieved with straight bars. Spalling was designed to induce bond degradation and hence anchorage failure of the flexural reinforcement, leading to a combined shear-bending failure of the component. Inserts to locally reduce the concrete cover were installed in the formwork prior to casting. The bespoke inserts were 3D printed to achieve the required dimensional accuracy. The reduction in cover was the same in the horizontal and vertical directions, measured respectively to the side face and underside of the beam. The dimensions and characteristics of the zone with cover reduction are shown in Figure 3. In the longitudinal direction, the anchorage length was 40 mm, equal to 5 times the bar diameter. This was achieved by using debonding sleeves either side of the bonded length, as shown in Figure 3.b.

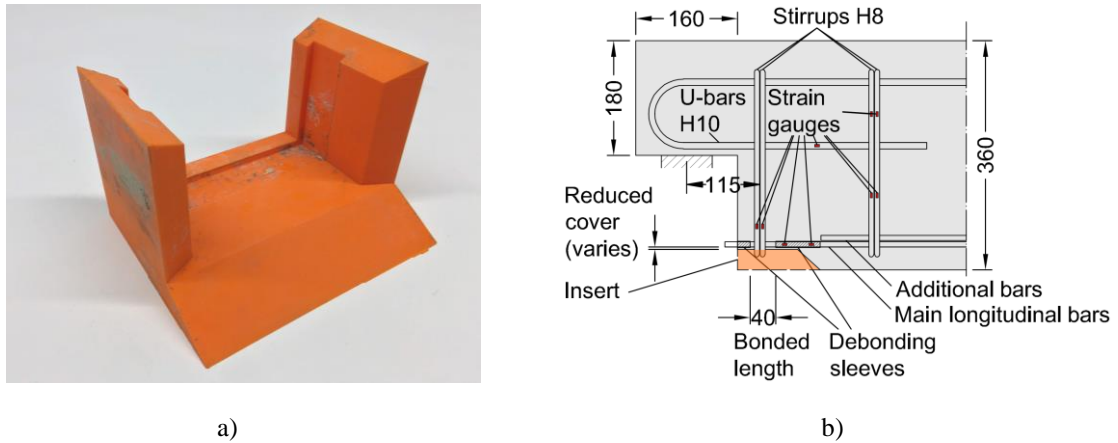


Figure 3. Simulated spalling on half-joint specimens: a) Sample of 3D printed insert; b) Schematic of anchorage zone, reinforcement details and location of strain gauges on the steel bars

3. Results

The load-deflection curves for all the tests are compared in Figure 4. The load values correspond to the vertical reaction under the half-joint nib. The value of the reaction was calculated as half of the central point load measured with the load-cell. The displacement was measured with a Linear Potentiometric Displacement Transducer (LPDT) at the top of the beam at the mid-span. All the specimens were tested up to failure.

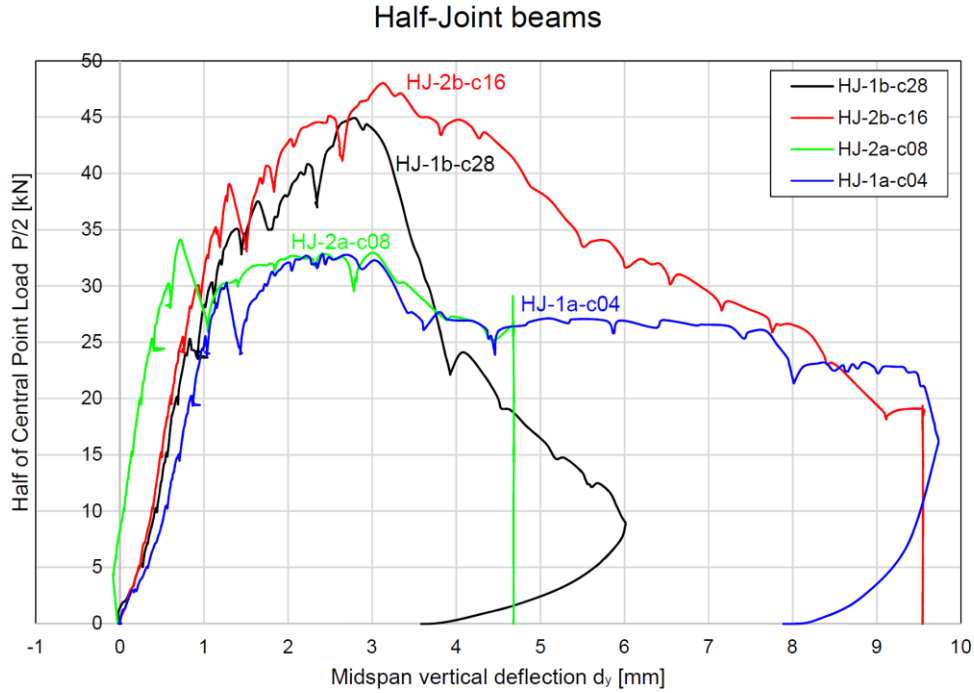


Figure 4. Comparison of load-deflection curves at the point of application of the central force.

Within the initial elastic range, the specimens exhibited slightly different initial stiffnesses, but no trend was identified. In terms of ultimate peak strength, HJ-1b-c28 failed at a load of 44.9 kN and HJ-2b-c16 failed at a slightly higher load of 48.0 kN. The half-joint HJ-2a-c08 and HJ-1a-c04 had peak loads of 34.1 kN and 32.9 kN respectively. The readings from the strain gauges located within the 70 mm unbonded length of the main longitudinal bars indicated that at peak loads, the bars reached average strains between $145 \mu\epsilon$ and $172 \mu\epsilon$, suggesting that the stresses in the steel remained well below the yield limit of the material. The cracking pattern of each half-joint after failure is shown in Figure 5. The cracks indicate that greater cover distances led to failure of the half-joint away from the anchorage region. Lower cover values led to anchorage failure of the longitudinal bars. The resulting slip of the bars induced the development of a diagonal crack originating at the bottom corner of the full-depth section (HJ-1a-c04, HJ-2a-c08, HJ-2b-c16). This was followed by multiple inclined cracks in the concrete compression zone, at the transition between the nib and the full-depth section.

4. Discussion

The cracking patterns and failure modes suggest that a cover distance of 28 mm was sufficient to withstand the anchorage demand of the node. Failure occurred elsewhere. The transition in behaviour appears to correspond to a cover distance between 28 mm and 16 mm. For lower values, failure occurred at the bottom corner. Even with low covers (HJ-1a-c04 and HJ-2a-c08), the specimens exhibited significant load bearing capacity, equal to 73-76% of that of the reference specimen (HJ-1b-c28). This can be attributed to the confinement provided by the transverse hanger reinforcement at the anchorage location. Where the longitudinal bars were fully exposed, slip resistance appeared to be provided through friction between steel and concrete, where the two materials were kept in contact thanks to the transverse reinforcement. Beyond the attainment of peak resistance, for large deformations and crack widths, the exposed segments of the reinforcement appeared to resist mainly through dowel action.

Where anchorage led to failure, cracking initiated from the bottom full-depth corner at approximately 45° . As the load increased, the main crack propagated with the same inclination until crossing the second row of vertical reinforcement, progressing with a steeper angle closer to the vertical direction. This can be characterised as a combined bending-shear behaviour. The crack

remained within a distance equal to a full-depth from the bottom corner, typically assumed to be the extent of the disturbed region of a half-joint (Desnerck et al. 2016). As the deformations and rotations increased, distributed cracking developed in the top compression zone. The development of inclined cracks in the full depth section leading to failure of the half-joint was also observed in the experimental programme by Desnerck et al. (2017), where the anchorage deterioration of the longitudinal bars was simulated with pre-cracked concrete cylinders around the bars or plastic sheets replicating horizontal cracking. The analogy between the results appears to confirm the vulnerability of the bottom node of the full depth section, and that deterioration of this node can trigger the overall premature failure of the component.

Where spalling of the concrete cover is due to corrosion of the steel reinforcement, the presence of corrosion products has an impact on the joint behaviour. As spalling was simulated without corrosion, this effect was not considered in the experimental programme. More research is necessary to investigate the effects of delamination and spalling together with other corrosion-induced phenomena, such as the presence of corrosion products, reduction in rib height and possible localised pitting corrosion.

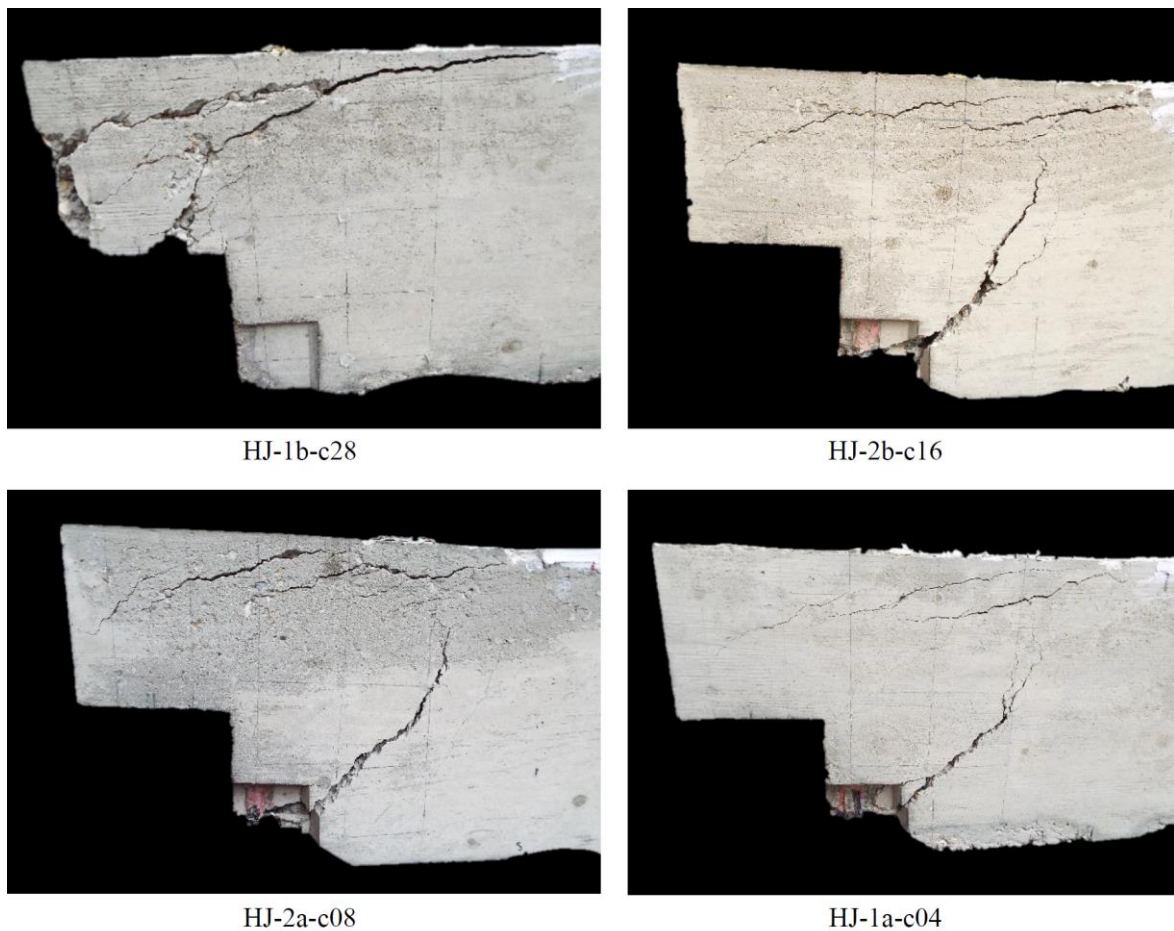


Figure 5. Cracking pattern of specimens after failure.

5. Conclusions

The following conclusions are drawn:

- In half-joints, the underside of the full-depth section does not benefit from the external confinement of direct support pressure. Hence, longitudinal tension bars in this region are vulnerable to anchorage deterioration;
- No correlation was found between the stiffness of the joints at working loads and their ultimate capacity;

- Reduced concrete cover led to a reduction in anchorage capacity of deformed steel bars at the bottom of the full-depth section;
- Anchorage failure at the bottom of the full-depth section led to combined bending-shear failure modes of the joint with a diagonal crack originating at the bottom corner;
- Where the cover distance was smaller than typical design provisions, the confinement due to the shear links provided some residual anchorage resistance to the longitudinal bars;
- Where anchorage was adequate, failure occurred away from the bottom corner;
- More research is necessary to investigate the behaviour of deteriorated half-joints in the presence of reinforcement corrosion.

Acknowledgements

The authors wish to express their gratitude to the staff of the University of Cambridge Structures Research Laboratory for their contribution to the experimental work presented here. The first author gratefully acknowledges the financial support of the United Kingdom Engineering and Physical Science Research Council (EPSRC) via a Doctoral Training Award [EP/M508007/1; EP/N509620/1].

References

- Cairns, J. (2015). Bond and anchorage of embedded steel reinforcement in fib Model Code 2010. *Structural Concrete*, 16(1), 45–55.
- Desnerck, P., Lees, J.M., and Morley, C.T. (2016). Impact of the reinforcement layout on the load capacity of reinforced concrete half-joints. *Engineering Structures*, 127, 227–239.
- Desnerck, P., Lees, J.M., and Morley, C.T. (2017). The effect of local reinforcing bar reductions and anchorage zone cracking on the load capacity of RC half-joints. *Engineering Structures*, 152, 865–877.
- Desnerck, P., Lees, J. M., Valerio, P., Loudon, N., and Morley, C.T. (2018). Inspection of RC half-joint bridges in England: analysis of current practice. *Proceedings of the Institution of Civil Engineers-Bridge Engineering*, 171(4), 290–302.
- di Prisco, M., Colombo, M., Martinelli, P. and Coronelli, D. (2018). The technical causes of the collapse of Annone overpass on SS. 36. *Proceedings of Italian Concrete Days 2018*, 13-15 June 2018, Lecco, Italy, 1–16
- fib* Bulletin 10 (2000), Bond of Reinforcement in Concrete. *Fédération Internationale du Béton (fib)*, Lausanne, Switzerland.
- Mak, M.W.T., Desnerck, P., and Lees, J.M. (2019). Corrosion-induced cracking and bond strength in reinforced concrete. *Construction and Building Materials*, 208, 228–241.
<https://doi.org/10.1016/j.conbuildmat.2019.02.151>
- Mak, M.W.T. and Lees, J.M. (2019). Bond degradation and reduced cover with transverse reinforcement. *Proceedings of the 1st fib Italy YMG Symposium on Concrete and Concrete Structures*, 15 October 2019, Parma, Italy. <https://doi.org/10.17863/CAM.44540>
- Mitchell, D., Marchand, J., Croteau, P. and Cook, W.D. (2011). Concorde overpass collapse: Structural aspects. *ASCE Journal of Performance of Constructed Facilities*, 25(6), 545–553.
- Orr, J.J., Darby, A., Ibell, T., Thoday, N., and Valerio, P. (2017). Anchorage and residual bond characteristics of 7-wire strand. *Engineering Structures*, 138, 1–16.
- Regan, P.E., and Kennedy Reid I.L. (2009). Assessment of concrete structures affected by cover delamination. Part 1: Effect of bond loss, *Studi e ricerche, Politecnico di Milano*, 29, 245–275.